FABRICATION OF *p*-NiO/*n*-ZnO:Ga HETEROSTRUCTURES FOR A RECTIFIER DIODE AND A UV PHOTODETECTOR VIA RF MAGNETRON SPUTTERING AND SPRAY PYROLYSIS SYNTHESIS

Lidia Ghimpu[1], Victor Suman[1], Dumitru Rusnac[2], and Tamara Potlog[2]

[1]D. Ghitu Institute of Electronic Engineering and Nanotechnologies, Academiei str.3/3, Chisinau, MD-2028 Republic of Moldova
[2]Moldova State University, A. Mateevici str. 60, Chisinau, Republic of Moldova
E-mail: lidia.ghimpu@gmail.com

(Received April 12, 2021)

https://doi.org/10.53081/mjps.2021.20-1.05 *CZU:535.33:543.4*

Abstract

In this paper, a *p–n* thin film NiO/ZnO heterojunction for a rectifier diode and a UV photodetector is prepared and characterized. Nickel oxide (NiO) and gallium-doped zinc oxide (ZnO:Ga) thin films are grown by RF magnetron sputtering and spray pyrolysis techniques, respectively. The crystal structure of the thin films is studied by the X-ray diffraction (XRD) method. The transmittance and reflectance are studied by UV–VIS spectroscopy. The *p–n* electrical parameters are estimated from current–voltage characteristics. The effects of duration of thermal annealing at 450°C on the characteristics of the NiO/ZnO:Ga device are evaluated. The non-annealed diode shows the best rectification coefficient of 10^5 at ±1 V. The *p–n* photodetection capability is studied under UV illumination. At a reverse bias of –3 V under 365-nm UV illumination, the device shows a current intensity of ~6.2×10^{-12} A. The observed increase in the reverse current intensity by about two orders of magnitude under a UV lamp with a spectral irradiance of 10 W m^{-2} μm^{-1} indicates a promising application in UV light detection.

Keywords: RF magnetron sputtering, spray pyrolysis, UV–VIS spectroscopy, electrical properties.

Rezumat

În această lucrare, a fost descrisă fabricarea și caracterizarea diodei redresoare și senzorului UV pe baza heterojoncțiunii cu straturi subțiri *p*-NiO/*n*-ZnO. Straturile subțiri de oxid de nichel (NiO) și oxid de zinc (ZnO:Ga) au fost obținute prin metoda pulverizării în regim de radiofrecvenţă (RF) și, respectiv, metoda pulverizării pirolitice. Structura cristalină a straturilor subțiri a fost investigată prin metoda difracției cu raze X (XRD). Transmitanța și reflectanța au fost studiate prin spectroscopie UV-VIS. Parametrii electrici ai heterojoncțiunii *p-n* au fost estimați din caracteristicile curent-tensiune. Au fost evaluate efectele duratei tratării termice la 450°C asupra caracteristicilor structurii NiO/ZnO:Ga. Dioda redresoare netratată a arătat cel mai bun coeficient de redresare de 10^5 la aplicarea tensiunii ±1 V. Capacitatea de detecție a senzorului pe baza heterojoncțiunii *p-n* a fost studiată la iluminarea UV**.** Curentul de întuneric al joncțiunii la polarizare inversă de -3V este ~ $6,2 \times 10^{-12}$ A. O creștere a curentului invers cu

aproximativ două ordine de mărime la iluminare cu lampa UV cu iradiere spectrală 10 $Wm^{-2}\mu m^{-1}$ prezintă o aplicație promițătoare în detectarea luminii UV.

Cuvinte cheie: pulverizare cu magnetron RF, piroliză prin pulverizare, spectroscopie UV–VIS, proprietăți electrice

1. Introduction

Metal oxide thin films have attracted much interest because of their electrical and optoelectronic characteristics and various applications. Zinc oxide and NiO have attracted attention as promising candidates for heterojunction thin film devices. The most important native defects that affect ZnO are attributed to the presence of interstitial zinc and oxygen and oxygen and zinc vacancies, which are intrinsic defects [1]. Niobium oxide is inherently of the *p*-type because of the presence of native acceptor defects generated by nickel vacancies. Both materials have good band alignment [2, 3]. Zinc oxide and NiO have been extensively studied for use in electronic and optoelectronic devices, such as light emitting diodes, sensors, photodetectors, and thin film *p–n* junctions [2–4]. The *p–n* type photodetector has many advantages, in particular, low bias current, high impedance, capability for high frequency operation, and compatibility of the fabrication technology with planar-processing techniques [5]. Up to now, a variety of *n*-type metal oxide thin films has been studied for *p–n* junction diode or ultraviolet (UV) photodetector applications. Among them, amorphous indium gallium zinc oxide (a-IGZO) has been widely studied because of its high mobility, good uniformity, low temperature process, and high optical transparency [6]. The amorphous nature of the IGZO thin film makes it a good choice for multi-layer devices due to the smooth interface, which is quite helpful to device performance [7]. Similar to *n*-type materials, *p*-type metal transparent oxides do not exist widely in nature. Among the available *p*-type metal oxide thin films, nickel oxide has been given considerable attention due to its *p*-type conductivity and transparency [8–11]. A UV detector based on lithium-doped NiO and ZnO was reported by Ohta et al. [12]. The literature survey reveals that there is no detailed report on analysis of the *p–n* junction parameter for gallium-doped ZnO and undoped NiO. In this paper, we describe the preparation and characterization of a heterojunction rectifier diode and a UV photodetector based on undoped NiO deposited by RF magnetron sputtering and Ga-doped ZnO grown by the spray pyrolysis technique.

2. Experimental

Nickel oxide deposition was conducted on a RF magnetron sputtering system using a Ni target of 99.5% purity. Nickel oxide was prepared at room temperature by RF magnetron sputtering at 210 W RF power. The distance from the sample to the target was 7–8 cm. The working pressure was maintained at 4×10^{-3} Pa. Different levels of carrier concentrations in the NiO layer can be achieved by introducing different amounts of O_2 gas during the sputtering deposition [13, 14]. With a higher amount of O_2 gas introduced during the sputtering deposition, a larger number of nickel vacancies, which act as acceptors, are formed in *p*-NiO thin films [13]; on the contrary, a smaller number of oxygen vacancies, which act as donors, are formed in *n*-ZnO thin films [14]. Zinc oxide layers doped with Ga were deposited by spray pyrolysis in an argon (Ar) atmosphere. The initial solution was prepared by dissolving zinc acetate $[Zn(CH_3COO)_2 \bullet 2(H_2O)]$ in a methanol–water solution in a ratio of 25 : 65 to obtain a concentration of 0.2 M. In addition, to prevent the aggregation process, a few drops of concentrated acetic acid were added to the starting solution. For doping of ZnO thin films,

gallium trichloride ($GaCl_3$) was used. The vacuum thermal annealing of ZnO:Ga thin films deposited on a NiO/glass substrate was performed at 450°C for 90 min. Heterojunctions having the structure of In/*n*-ZnO:Ga /*p*-NiO/Au were prepared in the following sequence. First, a 200-nm-thick NiO film was deposited on a glass substrate by the RF magnetron sputtering method. At 3–4 sccm O_2 (99.99%) in the O_2/Ar+O_2 flow, an RF power of 210 W, and a substrate temperature of 450°C, a carrier concentration on the order of 10^{16}–10^{17} cm^{-3} was achieved in the NiO thin film. After that, a 300-nm-thick ZnO layer doped with 3% Ga was deposited by spray pyrolysis. An Al electrode was evaporated for NiO, whereas Au was used for ZnO:Ga thin films.

The structural properties of NiO, ZnO:Ga, and NiO/ZnO:Ga thin films were studied at room temperature on *a XRD Rigaku* Ultima IV *diffractometer* using CuK_α radiation (λ = 1.5405 Å) at 40 kV and 30 mA. The optical transmittance values of the thin films were measured in a wavelength range of 300–900 nm using a PerkinElmer double-beam UV–VIS spectrophotometer. The current–voltage (I–V) measurements were conducted using a Keithley 2400 source meter and a Newport Oriel lamp (94023A).

3. Results and Discussion

Figure 1 shows X-ray diffraction pattern of the Ga-doped ZnO thin film thermally annealed in a vacuum and the NiO thin film grown at room temperature. The XRD studies of the ZnO:Ga thin film revealed a polycrystalline nature with the (0002) plane as the dominant orientation and a hexagonal wurtzite crystal structure, as confirmed by the standard JCPDS card number 089-1397. According to the authors of [15, 16], who studied Ga-doped ZnO thin films, the diffraction peak at 31.61^o indicate that Ga can occupy regular positions of the structure, while replacing zinc ions with tetrahedral coordination, or can be incorporated into octahedral interstices. We suppose that the observed diffraction peak corresponds to the $Zn_{1-x}Ga_xO$ phase [17]. The grain size estimated from the (0002) plane reached about 29.0 nm. The XRD results show that the NiO thin film has a polycrystalline structure with the (111) and (200) reflections corresponding to the NiO cubic lattice [18]. The average grain size of the NiO thin film is about 17.0 nm. At room-temperature growth, i.e., in the case of an unheated sample holder, the deposited atoms will have a lower mobility. This factor hinders the diffusion of atoms in an energetically convenient site and forces the atoms to nucleate in new sites of the atom; as a consequence, smaller grains are formed. The XRD pattern of the NiO/ZnO:Ga structure revealed the presence of not only ZnO and NiO phases, but also other phases, such as $NiGa_2O_4$ and NiO_2.

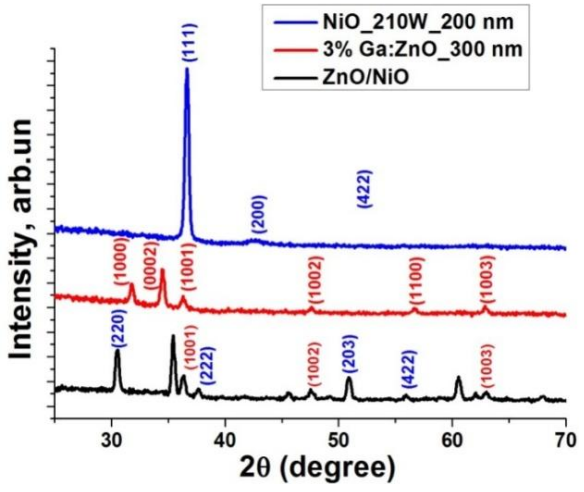

Fig. 1. X-ray diffraction pattern of the sputtered NiO thin film, the ZnO:Ga thin film thermally annealed in a vacuum, and the ZnO/NiO heterostructure.

It is well known that NiO exists in various oxidation states, such as nickel trioxide or sesquioxide (Ni_2O_3), nickelous oxide (NiO), nickel dioxide (NiO_2), nickelosic oxide (Ni_3O_4), and nickel peroxide (NiO_4). The ZnO XRD peaks are much weaker than those of NiO; this fact indicates that the ZnO thickness is ultrathin.

Table 1. Structural parameters of the sputtered NiO thin film, the ZnO:Ga thin film thermally annealed in a vacuum, and the ZnO/NiO heterostructure

Samples	**No.**	**2θ**	***d*, Å**	**FWHM, rad**	***D*, Å**	**ε**	**hkl**
NiO	1	36.64	2.4518	0.0068	236.70	0.00518	111
	2	42.60	2.1212	0.0246	67.22	0.01578	200
ZnO	1	31.79	2.8139	0.0065	242.91	0.00579	1000
	2	34.49	2.5996	0.0063	256.14	0.00507	0002
	3	36.30	2.4740	0.0075	214.62	0.00576	1001
	4	47.60	1.9097	0.0077	216.88	0.0044	1002
	5	56.69	1.6231	0.0085	204.05	0.00398	1100
	6	62.92	1.4766	0.0078	230.03	0.00321	1003
ZnO/NiO	1	30.51	2.9290	0.0067	236.52	0.00619	$NiGa_2O_4$220 (cubic)
	2	35.44	2.5320	0.0059	274.28	0.00462	unknown
	3	36.32	2.4727	0.0072	222.87	0.00555	ZnO 101
	4	37.65	2.3883	0.0063	255.61	0.00467	$NiGa_2O_4$222 (cubic)
	5	41.74	2.1633	0.0084	195.26	0.00554	unknown
	6	45.60	1.9887	0.0074	225.39	0.00441	unknown
	7	47.59	1.9101	0.0089	188.86	0.00506	ZnO 102
	8	50.91	1.7930	0.0073	231.20	0.00388	NiO_2 203
	9	55.94	1.6431	0.0076	227.23	0.00362	$NiAl_2O_4$ 422 (cubic)
	10	60.56	1.5283	0.0078	227.22	0.00336	unknown
	11	62.07	1.4947	0.0069	258.27	0.00289	unknown
	12	62.97	1.4755	0.0088	204.22	0.00361	ZnO 103
	13	67.95	1.3790	0.0076	241.43	0.00286	ZnO 112

The optical transmittance $T(\lambda)$ and reflectance $R(\lambda)$ spectra of the NiO, ZnO:Ga, and NiO/ZnO:Ga thin films in a wavelength range of 350–800 nm are shown in Fig. 2. These spectra show that the ZnO:Ga films exhibit a reflectance exceeding 20% in the visible range and a

transparency between 40–50% in the visible region. This low transparency can be attributed to the surface defects, such as voids and pores. The NiO thin film has a moderate transmittance in the short wavelength range of the UV–Vis region, which gradually increases in the NIR region. The transmittance of the NiO thin film in the visible region is between 30–40%. The transmittance of the NiO/ZnO:Ga structure is about 40% in the UV-VIS region; it gradually decreases in the NIR region. From the transmittance and reflectance spectra of ZnO:Ga, NiO, and NiO/ZnO shown in Fig. 2, the optical band gap was estimated by plotting the $(\alpha h\nu)^2 = f(h\nu)$ dependence. An extrapolation of the linear region to the photon energy axis allowed us to determine the bandgap energy, as shown in Fig. 3.

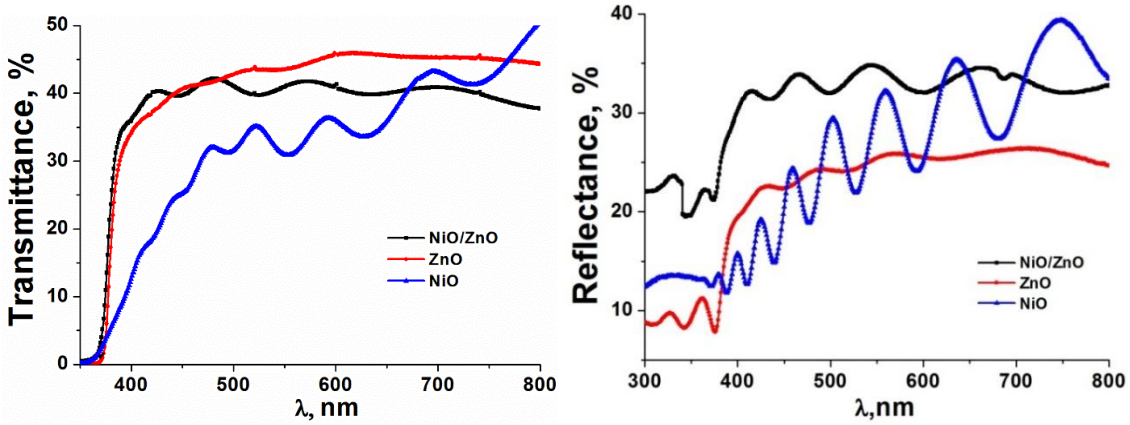

Fig. 2. Optical transmittance and reflectance spectra of the sputtered NiO thin film, the ZnO:Ga thin film thermally annealed in a vacuum, and the ZnO/NiO heterostructure.

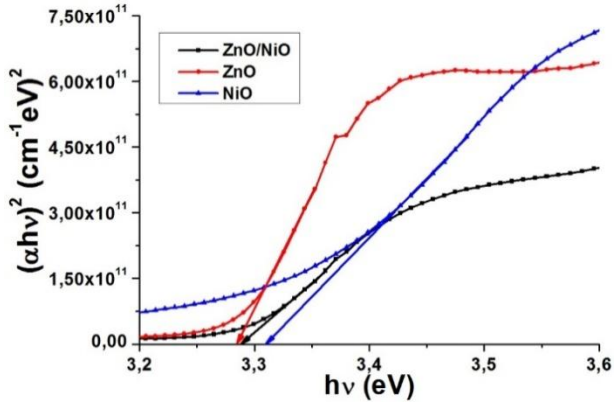

Fig. 3. The $(\alpha h\nu)^2 = f(h\nu)$ dependence of the sputtered NiO thin film, the ZnO:Ga thin film thermally annealed in a vacuum, and the ZnO/NiO heterostructure.

The optical band gaps of the ZnO :Ga, NiO thin films were calculated and indicated a direct transition. The band gap extracted from the $(\alpha h\nu)^2 = f(h\nu)$ dependence for the NiO thin film shows a value of 3.32 eV, while for ZnO:Ga and NiO/ZnO:Ga it shows the same value of

3.28 eV. The optical band gap values of these films are in the same range as those reported for bulk materials.

To study the effect of the thin film resistivity on the rectifying characteristics of the NiO/ZnO:Ga heterojunction, the ZnO:Ga thin films were annealed at 450°C in an O_2 atmosphere for different durations. As shown in Fig. 4a, an obvious tendency to decreasing can be observed for the forward current of the NiO/ZnO:Ga heterojunction with an increase in the annealing time. It is evident that annealing in an O_2 atmosphere causes an increase in the resistivity of the ZnO:Ga thin film. In addition, it is revealed that the longer the annealing time, the more resistant the ZnO:Ga thin film. If a forward bias is applied to the heterostructure, in addition to the voltage falling across the depletion region, part of the voltage will drop across the highly resistive ZnO:Ga region. In this case, it is reasonable to expect a smaller forward current. In addition, the highly resistive ZnO:Ga region also restricts the current passing through the entire heterostructure. Thus, a tendency to decreasing is observed for the forward current with an increase in the resistivity of the ZnO:Ga thin film. The best rectifying performance with a rectification coefficient of 10^5 at ±1 V was obtained for the NiO/ZnO:Ga heterojunction without annealing in an O_2 atmosphere.

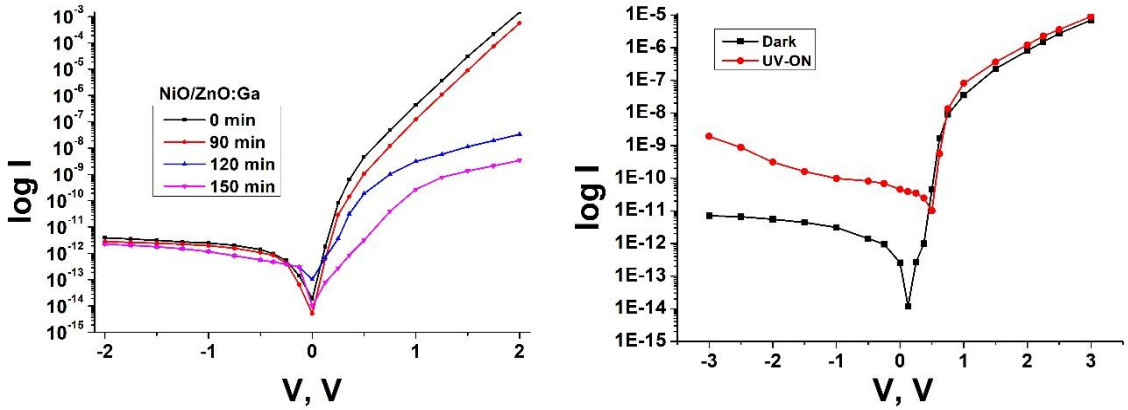

Fig. 4. (a) Current-voltage characteristics of the NiO/ZnO:Ga heterojunction with the ZnO:Ga thin film annealed in a vacuum for 0, 90, 120, and 150 min and (b) I–V characteristics under 365-nm UV light illumination for a heterojunction with the *non-annealed (0 min)* ZnO:Ga thin film.

Figure 4b illustrates the photoelectric response to the UV illumination of the *p*-NiO/*n*-ZnO:Ga heterojunction. The reverse dark current measured at –3 V is ~6.2×10^{-12} A. This finding shows the typical behavior of a *p*–*n* junction; that is, a higher acceptor concentration in the *p*-NiO layer leads to a lower reverse current. It is obvious that the UV illumination of the *p*-NiO/*n*-ZnO:Ga heterojunction causes an increase in the reverse current by about two orders and thereby shows a promising application in UV light detection. The phenomena could be attributed to the effect of the UV-induced hole trapping in the *p*-NiO layer. The UV illumination produces electron–hole pairs in both the *p*-NiO and *n*-ZnO:Ga layers. If some of the UV-generated holes are trapped in the deep-levels in the *p*-NiO layer, the I–V characteristic of the *p*-*n* junction will be affected by the hole trapping. The hole trapping will partially compensate for the negative space charge in the *p*-NiO side of the depletion region of the *p*–*n* junction, while reducing the built-in electric field and the barrier height of the *p*–*n* junction.

4. Conclusions

Thus, the *p*-NiO/*n*-ZnO:Ga thin film heterojunctions have been prepared for both rectifier diode and UV photodetector applications. For the diode application, the conductivities of both the NiO and ZnO:Ga thin films have a strong effect on the rectifying characteristic of the heterojunction diode. The best rectifying performance has been obtained for the diode with both highly conductive NiO and ZnO:Ga thin films. The evolution of the electrical properties studied by the I–V measurements has shown that vacuum annealing suppresses the rectifying nature of the annealed heterojunctions. The photocurrent to dark current ratio for the *p*-NiO/*n*-ZnO:Ga thin film heterojunction upon applying a 1 V reverse bias is about 35.

Acknowledgments. The authors thank the Ministry of Education, Culture, and Research of the Republic of Moldova for funding the research (grant 20.80009.5007.02).

References

[1]S. P. Ghosh, K. C. Das, N. Tripathy, G. Bose, et al., IOP Conf. Ser.: Mater. Sci. Eng. 115, 012035 (2016).
[2]N. Park, K. Sun, Z. Sun, Y. Jing, and D. Wang, J. Mater. Chem. C. 1, 7333 (2013).
[3]S. Huang, N. Yu, T.Wang, and J. Li, Func. Mater. Lett. 11, 1850045 (2018).
[4]A. Adhikary, S. Ahsan, M. Hossain, B. Hossain, S. Newaz, F. Ahmed, and Ik-Bu Sohn, Opt. Eng. 59, 117108 (2020).
[5]K.Dy, J. Ryu, J. Manders, J. Lee, and F. So, Appl. Mater. Interfaces 6, 1370 (2014).
[6]P. Liu, T. P. Chen, X. D. Li, Z. Liu, J. I. Wong, Y. Liu, and K. C. Leong, ECS Solid State Lett. 2, Q21 (2013).
[7]K. Kobayashi, M. Yamaguchi, Y. Tomita, and Y. Maeda, Thin Solid Films 516, 5903 (2008).
[8]H.-L. Chen, Y.-M. Lu, and W.-S. Hwang, Surf. Coat. Technol. 198, 138 (2005).
[9]P. Salunkhe et al., Mater. Res. Express 7, 016427 (2020).
[10] M. Yang, H. Pu, Q. Zhou, and Q. Zhang, Thin Solid Films 520, 5884 (2012).
[11] H. Lee, Y. T. Huang, M. W. Horn, et al., Sci. Rep. 8**,** 5590 (2018).
[12] H. Ohta, M. Hirano, K. Nakahara, H. Maruta, T. Tanabe, M. Kamiya, T. Kamiya, and H. Hosono, Appl. Phys. Lett. 83, 1029 (2003).
[13] H. K. Li, T. P. Chen, S. G. Hu, X. D. Li, Y. Liu, P. S. Lee, X. P. Wang, H. Y. Li, and G.. Q. Lo, Express 23, 27683 (2015).
[14] E. Chong, Y. S. Chun, S. H. Kim, and S. Y. Lee, El. Eng. Technol. 6, 539(2011).
[15] M. Razeghi, J. H. Park, R. McClintock, D. Pavlidis, F. H. Teherani, D. J. Rogers, B. A. Magill, G. A. Khodaparast, Y. Xu, J. Wu, et al., Proc. SPIE, 10533 (2018).
[16] H. Aida, K. Nishiguchi, H. Takeda, et al., Jpn. J. Appl. Phys. 47, 8506 (2008).
[17] S. Annathurai, S. Chidambaram, M. Rathinam, and G. K. Prasanna Venkatesan, J. Mater. Sci.: Mater. Electron. 30, 5923 (2019).
[18] N. Park, K. Sun, Z. Sun, Y. Jing, and D. Wang, J. Mater. Chem., C 1, 7333 (2013).